Analysis of a non-calorimetric method for assessment of in-situ thermal transmittance and solar factor of glazed systems

Francesco Goia[1,*] and Valentina Serra[2]

[1] *Department of Architecture and Technology, Faculty of Architecture and Design, Norwegian University of Science and Technology, NTNU, Trondheim, Norway*

[2] *TEBE Research Group, Department of Energy, Polytechnic University of Turin, Torino, Italy*

** Corresponding author's contact: e-mail: francesco.goia@ntnu.no / telephone: +47 45 02 74 37*

Abstract

The performance of glazing systems is usually assessed through the thermal transmittance and the solar factor, two metrics characterised either through calorimetric laboratory tests or calculations. In this paper, the analysis of the performance of a non-calorimetric method for obtaining the in-situ thermal transmittance and solar factor of glazing systems is presented. This method, developed as a trade-off between accurate (and expensive) laboratory tests (which characterise the systems under standardised, "averaged" conditions), and easy and less expensive tests on systems installed in real buildings (under real operative conditions), has been previously adopted for the characterisation of different glazed systems, but never presented and discussed in full detail.

The method, suitable for full-scale glazing systems installed in buildings or in test cells, is based on the acquisition of temperature, heat flux, and solar irradiance values. Experimental data is then processed through simple equations and linear regressions to determine the thermal transmittance and the solar factor under real boundary conditions. In this paper, a detailed description of the method, the experimental test rig, and the related expected accuracy is reported. The method is then applied to a case study (a conventional double glazed unit) to give an example of the proposed procedure and to validate it.

The results of the case study show the capability of the assessed in-situ thermal transmittance and solar factor to replicate the thermophysical behaviour of the glazing system within a satisfactory degree of accuracy. An in-depth discussion on the observed outcomes from the case study deepens the understanding of the method's performance and the results' significance.

Keywords: *thermal transmittance; solar factor; in-situ assessment; glazing.*

Highlights

- Details of an in-situ assessment method for U-value and g-value are given.
- The method is tested on a case-study (Double Glazed Unit) for reliability check.
- Performance gap between nominal and in-situ performance of glazing is analysed.

Nomenclature

Symbol	*Quantity*	*Unit*
A	Surface area	m^2
DD	Degree day	°C day
dq	Specific heat flux	W/m^2
e	Experimental value	W/m^2 or Wh/m^2
E	Specific solar irradiance	W/m^2
e_n	Normalised residual	-
g (g-value)	Solar factor	-
G_{24}	Specific daily solar irradiation	J/m^2
h	Heat transfer coefficient	W/m^2 K
q	Specific heat	J/m^2
R	Thermal resistance	$(m^2$ K)/W
R^2	Coefficient of determination	-
RMSE	Root Mean Square Error	W/m^2 or Wh/m^2
s	Simulated value	W/m^2 or Wh/m^2
t	Time	s
T	Temperature	° C
U (U-value)	Thermal transmittance	W/m^2 K

Greek symbol

$\lvert\varepsilon_{\%}\rvert$	Absolute percentage error	%
Δt	Time interval	s
ΔT	Temperature gradient	° C
Λ	Thermal conductance	W/m^2 K
ρ	Reflectance	-
τ	Tranmsittance	-

Superscript

$\bar{}$	Referred to the in-situ quantity
$\hat{}$	Referred to the expected value

Subscript

c	Referred to convection
diff	Referred to the diffuse component
ΔT	Referred to the temperature gradient
esp	Referred to the experimental datum
e	Referred to the outdoor / solar spectrum
g	Referred to the solar irradiation / glased surface
i	Referred to the indoor / secondary transmission / i- element of a summation
E	Referred to the secondary transmission
in	Referred to the indoor
ind	Referred to the indirect component
op	Referred to the opaque surfaces
out	Referred to the outdoor
r	Referred to radiation
sim	Referred to the simulated datum
TOT	Referred to the total quantity

1. Introduction

Glazing systems play an important role in the building envelope in assuring not only a high energy performance, but also high user satisfaction when it comes to visual environment and comfort. It is therefore not surprising that the trend in architecture is to have more and more glazed surfaces in buildings, and the corresponding vibrant research and development activity to assure that highly transparent building envelops can be realised without impairing, and even enhancing, the energy and environmental performance of the façade.

The characterisation of the behaviour of glazed system is therefore an important part of the assessment of the overall performance of the building. When it comes to energy performance characterisation, a glazed system is conventionally modelled through two steady-state, simplified performance parameters: the thermal transmittance (*U-value*, [W/m^{2}K]) and the solar factor[1] (*g-value*, [-]). These two values can be obtained through laboratory tests and sub sequential calculations, or through software tools that integrate databases of glass panes.

The aim of these metrics, which are calculated assuming a standardised, average situation for glazing in practice, is to allow a fair comparison between different products to be made. Furthermore, they are widely used in calculation methods for the assessment of the annual energy use for space heating and the cooling of a residential or a non-residential building (ISO 13790, 2008), which form the basis for the energy performance certificate of a building in many European countries.

On the one hand, these simplified metrics are useful during the design phase to select among different alternatives, based on the expected performance pictured by the U-value and the g-value. On the other hand, it is important to highlight that heat and solar transmission though a glazed system when placed under real operative conditions may differ to a relatively large extent from those pictured through the standardised metrics. This fact can be explained considering the following simplifications adopted in the standardised calculation procedures.

- Steady state heat flux; which in the characterisation/calculation of the thermal transmittance leads to neglecting thermal inertia effect of the glazed layer(s). If this assumption is quite reasonable for a thin,

[1] Also called Total Solar Energy Transmittance (TSET), or Solar Heat Gain Coefficient (SHGC).

single glass pane, multiple glazing characterised by thicker panes (e.g. with security, laminated glass panes) may present non-negligible dynamic heat transfer phenomena, which can lead to a shift in the peak transmitted heat flow higher than 1 h.

- Standardised and constant convective and radiative heat transfer coefficients towards the outdoor and indoor environment, which impact on both the value of the thermal transmittance and on the secondary heat transfer factor towards the inside, a quantity necessary in the calculation of the solar factor. In particular, the wind velocity on the outside surface is set to 4 m/s, a value that corresponds to quite high windy conditions. These assumptions lead,to a value for h_e in the range 23 to 25 W/(m^{2}K) and for h_i in the range 7.7 to 8 W/(m^{2}K) for a vertical window, depending on the adopted standard.
- Electromagnetic (solar) radiation (nearly) impinging perpendicularly on the glazed system. This assumption disregards any angle-dependent feature of radiation transfer through the transparent component. While this assumption is reasonable within a certain range of impinging angles close enough to the normal to the pane's surface, it may differ substantially when the real geometric relationship between a (vertical) window and the sun (and the sky dome) are considered. This is particularly true in moderate and low latitude locations, and especially in summer time.

The discrepancy between the boundary conditions registered in-situ and standardised values may lead to substantial differences between the calculated and in-situ energy performance of the glazed system, especially when the transparent envelope's performance is obtained through simplified metrics and not fully dynamic calculation methods.

In this paper, a non-calorimetric method for the characterisation of in-situ thermal transmittance and solar factor of glazed systems is reported. This procedure has been previously adopted in experimental campaigns on triple glazed units with an integrated shading system (Favoino et al., 2016) and on triple glazed units with/without smart glass panes (Bianco et al., 2017a, 2017b), to assess both the in-situ thermal transmittance and solar factor; and on a double glazed system (Goia et al., 2014b) to assess the in-situ thermal transmittance, and on thermotropic glass panes (Bianco et al., 2015). Furthermore, parts of this methodology have also been previously used for assessing the different energy performance of advanced glazed façades in office buildings

(Bianco et al., 2013; Goia et al., 2014a). However, this methodology has never been presented with full details and its potential and limitations not discussed. The aim of this non-calorimetric method is to provide an experimental procedure, which presents a trade-off between complexity, costs, and accuracy, to assess the energy performance of full-scale glazed system installed either in outdoor test cells or in a real building. The target accuracy of the method lies around of ± 10 % to 15 %, and costs to in the range of EUR 2000 to EUR 3000 for the entire measurement chain (sensors and data acquisition system).

In the context of this paper, the terms thermal transmittance and solar factor, where not differently specified, and refer to the values derived under in-situ conditions, and therefore not according to the standardised assumptions described above – and are provided in the long list of relevant international technical standards (EN 410, 2011; EN 673, 2011; EN 674, 2011; EN 675, 2011; ISO 9050, 2003; ISO 10077, 2017; ISO 10291, 1994; ISO 10292, 1994; ISO 10293, 1997). In order to highlight that the values of the metrics obtained in this paper refer to real, in-situ boundary conditions, both the thermal transmittance and the solar factor are identified with a bar above the usual symbol: $\bar{U}$ [W/m^{2}K] for the in-situ (or equivalent) thermal transmittance and $\bar{g}$ [-] for the in-situ (or equivalent) solar factor.

The reason to develop a simple, yet robust procedure to identify the in-situ, equivalent thermal transmittance, $\bar{U}$ and the in-situ, equivalent solar factor, $\bar{g}$ lies in the need of establishing experimental methods that allow the assessment of envelope technologies under real operations to be carried out. This is particularly useful not only for R&D activities on glazed systems, but also in the framework of building energy audit procedures and post-construction monitoring of energy and environmental performance of a building.

2. Background

2.1. Simplified models for heat transfer calculation in transparent systems with *U-value* and *g-value*

U-value and the g-value are at the basis of the calculation of heat transfer through transparent components in the most common calculation procedures. Using a rather simplified model[2], at any given time, the total heat

[2] Yet at the basis of many computational approaches, among which those reported in the (ISO 13790, 2008).

flow density dq [W/m^2] through the glazed part of a façade, from the outside of the building to the inside of the building, is given by the simple equation here below (Eq. 1), where E_{out} [W/m^2] is the global solar irradiance impinging on the façade, T_{in} is the indoor air temperature and T_{out} is the outdoor air temperature.

$$dq = E_{out} \cdot g - U \cdot (T_{in} - T_{out}) \text{ [W/m}^2\text{]} \quad (1)$$

For a given time interval [y; z], the total heat per m^2 of glazed surface that crosses the façade is given by the Equation 2, where t is the time, which can be further simplified to Equation 3 if U-value and g-value are time-independent variable:

$$q = \int_y^z E_{out}(t) \cdot g(t) - U(t) \cdot (T_{in}(t) - T_{out}(t))dt \text{ [J/m}^2\text{]} \quad (2)$$

$$q = g \cdot \int_y^z E_{out}(t)dt - U \cdot \int_y^z (T_{in}(t) - T_{out}(t))dt \text{ [J/m}^2\text{]} \quad (3)$$

This short recall about the use of the thermal transmittance and solar factor for calculation of the total heat flow or heat transfer through a glazed system is functional to the validation process carried out in Section 4.

2.2. State of the art of experimenatal and numerical procedures for characterisation of U-value and g-value

The experimental and numerical techniques for the determination of the U and g values have been established and standardised for a couple of decades and are routine procedures in research institutions and in the industry that allow catalogue properties to be assessed.

The determination of the standardised thermal transmittance of single or multiple glazing system can be carried out by means of two methods, the guarded hot-plate method (EN 674, 2011; ISO 10291, 1994; ISO 10292, 1994) and the heat-flux meter (EN 675, 2011; ISO 10293, 1997). These procedures make use of two items of laboratory equipment, the guarded hot-plate apparatus (ISO 8302, 1991) and the heat-flux meter apparatus (ISO 8301, 1991), to determine the thermal resistance R of the glazing system. In both cases, the apparatus is placed vertically to assure a horizontal heat flux through the glazed system under test. The total thermal transmittance U is then calculated (Eq. 4) by adding to the measured thermal resistance the internal and external surface resistances correspondent to the standardised internal (h_i = 7.7 or 8 W/m^{2}K, depending on the standard) and external (h_e = 23 or 25 W/m^{2}K, depending on the standard) surface heat transfer coefficients, which account for both radiative and convective heat exchange with the surrounding environments.

$$U = \frac{1}{h_i} + R + \frac{1}{h_e} \text{ [W/m}^2\text{K]} \quad (4)$$

The determination of the g-value is also composed by an experimental and a numerical element, as described in the two available international technical standards (EN 410, 2011; ISO 9050, 2003) for the determination of the solar factor (there called total solar energy transmittance). The solar factor g is the sum of the solar direct transmittance τ_e [-] and the secondary heat transfer factor q_i towards the inside (Eq. 5), the latter resulting from heat transfer by convection and longwave IR-radiation of that part of the incident solar radiation which has been absorbed by the glazing.

$$g = \tau_e + q_i \text{ [-]} \quad (5)$$

The solar direct transmittance is obtained by spectrophotometric measurements with nearly perpendicular impinging angle of the electromagnetic radiation on single glass panes, as described in (EN 410, 2011; ISO 9050, 2003), and followed by calculations to assess inter-pane reflection in case of multiple glazing. The secondary heat transfer factor is numerically determined (for single glass panes and for multiple glazing) through a series of assumptions on the surrounding environments.

These mentioned characterisation procedures are employed in laboratories with glazing samples in the range of 100 (for optical characterisation) to 800 mm (for thermal characterisation). When it comes to full-scale components, only one standardised procedure is available (ISO 12567-1, 2010), and concerns the determination of the thermal transmittance of a complete window (thus including also the non-transparent parts) through a calibrated hot-box apparatus, and a test rig defined in (ISO 8990, 1994). In-situ characterisation of the thermal transmittance of a glazed system is not described in any technical standard, though a procedure for in-situ assessment of thermal transmittance of opaque building envelope components is available (ISO 9869-1, 2014), and makes use of the heat-flux meter method. However, the direct translation of this standard procedure to in-situ assessment of the thermal transmittance of glazed system is not straightforward. While the influence of the solar irradiance on the heat-flux meter measurement is corrected in the method for opaque components through

the use of the moving average technique[3], the transparent feature of glazed systems makes it extremely complicated to fully avoid any interference of solar radiation on the measures.

The assessment of the solar factor on a full-scale glazed system (either in laboratory or in-situ) is not a standardised procedure. However, this type of characterisation is expected to become more and more fundamental, especially when moving from simple glazed technologies to more advanced ones, characterised by asymmetrical features (e.g. glazed systems integrating venetian blinds). Recently, the American National Fenestration Rating Council (NFRC) has proposed a procedure (NFRC 201, 2017) to assess the solar factor through a calorimetric method that makes use of a hot-box-like facility.

Aside from standardised techniques, researchers have developed laboratory procedures for the assessment of the solar factor through different measurement techniques.

In a reference paper by Kuhn, detailed descriptions of procedures based on more than twenty-five years of experience in g-value testing at Fraunhofer ISE (Freiburg, Germany) are reported (Kuhn, 2014). In the paper, two procedures for the calorimetric measurement of g under steady-state laboratory conditions are illustrated: the "Cooled plate method" and the "Cooled box method". The corresponding error analysis and methods to correct experimentally determined values of the solar factor to reference conditions (when it is not possible to reproduce the reference boundary conditions exactly in the laboratory) are reported too.

More recently, improved approaches for the determination of the solar factor in outdoor test cell facilities have been suggested in a paper (Pagliano et al., 2017), where dynamic (natural) boundary conditions are used in place of steady-state conditions to characterise through a calorimetric method in the in-situ solar factor $\bar{g}$.

In the paper, two new strategies to extract and measure the solar load entering through a full-scale glazed system are presented, and the new design concept of test cell facility to carry out such a procedure is illustrated. The simulations behind the study suggest that, compared to a traditional solution, the two proposed procedures offer a higher measurement accuracy and measurement precision in the determination of the solar factor.

[3] Through this approach, not only the influence of solar irradiance is reduced, but also those of not-stable indoor and outdoor air temperatures. However, the effect of temperature fluctuation is usually much less relevant than that due to the impinging solar irradiance.

To the best knowledge of the authors, and after a careful literature and standards' review, there are not standardised or recommended procedures for in-situ assessment of $\overline{U}$ and $\bar{g}$, and the only existing guidelines refer to testing in indoor or outdoor test cells with calorimetric features. On the one hands these methods and procedures are leading to accurate results, on the other hand they results to be inapplicable in real buildings and for glazed systems under real operations, where a calorimetric apparatus cannot be installed.

3. Methods

3.1. Physical quantities, sensors, and accuracy

The physical quantities to be measured in order to characterise the in situ thermal transmittance and solar factor are listed here below, and schematised in Fig. 1.

- The outdoor and indoor air temperature, hereafter indicated as T_{out} [°C] and T_{in} [°C], respectively.
- The area specific outdoor global (on the window plane) and indoor global (on the window plane) solar irradiance, hereafter indicated as E_{out} [W/m^2] and E_{in} [W/m^2], respectively.
- The area specific heat flow exchanged by convection and radiation between the inside facing glass pane of the glazed system and the indoor environment, are hereafter indicated as $dq_{c+r,in}$ [W/m^2].

Additional physical quantities that might be measured for control purpose – but are not mandatory for the proposed method – are:

- the surface temperature of the outside facing and inside facing glass panes of the glazed system [°C];
- the area specific heat flow exchanged by convection and radiation between the outside facing glass pane of the glazed system and the outdoor environment [W/m^2];
- the area specific diffuse solar irradiance in the indoor environment, measured on the vertical plane of the glazing system under test [W/m^2]

Figure 1

Surface and air temperatures should be measured with relatively fast-response sensors. Thermocouples and RTD sensors are, in the experience of the authors, adequate contact sensors to carry out the task. The accuracy of the sensors (together with the entire measurement chain) should be equal or higher than ± 0.3 °C in order to

assure a sufficient measurement quality. Both surface and air temperature sensors should be shielded by the influence of solar irradiation and suitably ventilated in order to assure a correct reading.

The area specific global solar irradiance values should be measured with thermopile pyranometer compliant methods with the relevant standard (ISO 9060, 1990), and preferably with a first-class (or higher accuracy) pyranometer. However, a second-class pyranometer might still represent an acceptable trade-off between accuracy and cost of equipment. The calculation of the total accuracy of the sensor for solar radiation measurement is not a straightforward process, as the accuracy is influenced by several factors (non-stability, non-linearity, directional response, temperature response, tilt response, spectral selectivity) that do not only depend on the sensor itself, but also on the time of the measurement and the location of the measurement (solar geometry). Presently, there is not a standardised method nor is there international consensus on uncertainty evaluation of pyranometer measurements under real operations, and manufacturers provide estimates of achievable uncertainties of measurements with their own instruments. For example, a leading manufacturer for thermal sensors estimates the achievable uncertainties of measurements (hourly total irradiance value, based on 1 s sampling), carried out at mid-latitude locations with its sensors (the same sensors used in the case study presented in Section 4) to be, depending on the season, in the range 3% to 5% and in the range 5% to 9%, for first-class pyranometers and second-class pyranometer, respectively (Hukseflux, 2016).

As far as the measurement of the solar irradiance transmitted through the system is concerned, it is necessary to point out that the value read by the pyranometer placed closed to the on the indoor side of the glazing systems (Fig. 1, sensor 3) is influenced by the diffuse indoor solar irradiance reflected back towards the inside by the glazed system. The impact of this effect on the measurement of the transmitted solar irradiance is hard to assess in general terms, because it depends to a great extent on the type of glazing system, on the geometry and the optical properties of the room where the measurement is carried out. A possible solution by which to take into account this influence is to measure the diffuse solar irradiance in the room (by means of an additional pyranometer placed right next the one for the transmitted irradiance, but facing towards the inside, such aa sensor 9 in Fig. 1). This recorded datum should then be multiplied by the indoor-side reflection coefficient (from technical datasheet or using average values for glazing type) of the system, and the resulting value

subtracted by the total reading of the pyranomenter that measures the transmitted solar irradiance (sensor 3 in Fig. 1). Alternatively, the diffuse solar radiation of the indoor environment can be estimated or simulated, based on the geometrical and optical characteristic of the room, and the correction can be carried out using such an estimation. However, as explained in the Discussion section, the actual amount of indoor diffuse solar irradiance back-reflected by the glazing system and read by the pyranometer is almost always lower than two orders of magnitude of the directly transmitted irradiance. This eventually leads to consider this contribution negligible in the framework of the aims of the proposed method.

The area specific heat flow exchanged by convection and radiation between the inside-facing glass pane and the indoor environment can be measured by means of a heat flow meter. The accuracy for this type of sensor may vary greatly because of a series of contributions (calibration uncertainty, resistance error, deflection error, temperature dependence, sensor's stability), and again on the type of measurement (where the heat flux is measured). Under ideal conditions, a high quality heat flux meter can assure measurements of heat flux in building physics applications in the range ± 5 %, as declared by manufacturers.

For reference purposes, it is interesting to report that the relevant technical standard for measurement of thermal resistance (ISO 9869-1, 2014) shows examples where the uncertainty budget includes contributions from temperature measurements and dynamic effects, leading to typical uncertainties in the order of ± 20 % for on-site measurements of thermal resistances according to the procedure presented in the standard.

When used in connection to glazed systems, heat flux meters need to be shielded by the effect of solar irradiation. For this purpose, thin reflective foils should be placed on the outside facing surface of the glazed system so that they shadow the heat flux meters (placed instead on the inside facing surface of the glazed system). If on the one hand this procedure reduces locally the solar radiation absorbed by the glass, on the another hand it is the best compromise between minimising solar influence on the sensor (during the daytime) and introducing a local change in the thermophysical properties of the system.

Another necessary observation about the use of heat flux meters deals with the increase in the thermal resistance of the glazing system where the heat flux is measured due to the sensor itself. The thermal resistance of a heat flux meter varies depending on the type of sensor, but common values for high-quality heat flux meters

are in the range 2×10^{-3} to 8×10^{-3} (m^2 K)/W. The total thermal resistance of a conventional double glazed unit is usually greater than 4×10^{-1} (m^2 K)/W, and the thermal resistance of more high-performance glazed unit is far higher and can reach value higher than 1 (m^2 K)/W. This in turn means that the thermal resistance of a glazed unit is at least two order of magnitude greater than that of the sensor. Such a large difference assures that the contribution of the additional thermal resistance introduced by the sensor is negligible when compared to the original thermal resistance of the glazed system (and fully within the target uncertainty of the method).

Considering a set of instruments composed by thermometers, with absolute accuracy of ± 0.3 °C, pyranometers with total relative accuracy (in a conservative case) of 9%, and heat flux meters with total relative accuracy of ± 5 %, the following uncertainties for the equivalent thermal transmittance $\bar{U}$ and equivalent solar factor $\bar{g}$ are found: ± 7 % and 16 %. These refer to an instantaneous value of the above mentioned physical quantities, which are to be recorded with a sub-hourly rates. Sampling in the range around 30 s can be considered a sufficient compromise when it comes to fast-changing quantities (solar irradiance and air temperature), while the sampling of quantities with longer time-constant (surface temperatures and heat flux) can be carried out with a longer time-step (higher than 1 min). Data can be then averaged in order to obtain longer time-steps (e.g. hourly step) to carry out the data processing to carry out the presented procedure.

3.2. Performance parameters' definition and data processing

Both the parameters $\bar{U}$ and $\bar{g}$ are to be obtained by linear regression, carried out with the well-known Ordinary Least Squares method (Hutcheson, 1999), imposing that the dependent variable is 0 when the independent variable is 0.

$\bar{U}$ is assessed by making use of night-time readings only, when there is no solar radiation impinging on the glazing, by directly correlating (Eq. 6) the reading of the heat-flux meter (dq) and the difference between the measured outdoor and temperature and the measured indoor air temperature (ΔT, Eq. 7). The need to use only night-time readings is due to the fact that, as per definition of the thermal transmittance, there cannot be heat generation within the assembly – an effect that instead occurs under solar irradiation because of the absorption of the glass panes.

$$\bar{U} = \left[\sum_i^n \left(\Delta T_i \cdot dq_i\right)\right] \cdot \left[\sum_i^n \Delta T_i^2\right]^{-1} \quad (6)$$

$$\Delta T = \left[T_{out} - T_{in}\right] \quad (7)$$

The assessment of the equivalent solar factor $\bar{g}$, carried out using day-time readings only, is also the result of a linear regression (Eq. 8). However, some calculation steps are necessary before the linear regression is performed, in order to decouple the heat flux released at the indoor interface because of the thermal gradient between outside and inside ($dq_{\Delta T}$ [W/m^2]) and the heat flux realised towards the inside because of the secondary transmittance (dq_I [W/m^2]) of the glazing. In particular, total transmitted solar flux dq_g [W/m^2] (which includes the contribute of the direct transmitted irradiance E_{in} and of the secondary transmitted flux dq_I) needs to be calculated (Eq. 9) by removing from the acquired total surface heat flux (dq) the contribution of the heat flux released at the indoor interface ($dq_{\Delta T}$) because of the thermal gradient between outside and inside (Eq. 10). The latter is calculated (Eq. 11) assuming the system is in a steady-state and is using the equivalent thermal transmittance obtained thorough linear regression mentioned above (Eq. 6).

$$\bar{g} = \left[\sum_i^n \left(E_{out,i} \cdot dq_{g,i}\right)\right] \cdot \left[\sum_i^n {E_{out,i}}^2\right]^{-1} \quad (8)$$

$$dq_g = \left[E_{in} + dq_E\right] \quad (9)$$

$$dq_E = dq - dq_{\Delta T} \quad (10)$$

$$dq_{\Delta T} = \bar{U} \cdot \Delta T \quad (11)$$

The goodness of the fit between the data set and the regression line, both in the case of the $\bar{U}$ and of the $\bar{g}$, can be assessed by means of the coefficient of determination R^2 [-], whose analytical formulation is given here below for the in-situ thermal transmittance (Eq. 12) and the in-situ solar factor Eq. 13).

$$R^2 = 1 - \left\{\left[\sum_i^n \left(dq_i - \Delta T_i \cdot \bar{U}\right)^2\right] \cdot \left[\sum_i^n \left(dq_i - n^{-1} \cdot \sum_i^n dq_i\right)^2\right]^{-1}\right\} \quad (12)$$

$$R^2 = 1 - \left\{\left[\sum_i^n \left(dq_{g,i} - E_{out,i} \cdot \bar{g}\right)^2\right] \cdot \left[\sum_i^n \left(dq_{g,i} - n^{-1} \cdot \sum_i^n dq_{g,i}\right)^2\right]^{-1}\right\} \quad (13)$$

4. Case study

A case study is presented in this paper in order to show the application of the proposed method, and to test its applicability. The in-situ thermal transmittance and solar factor have been assessed for a simple, full-scale glazed system, installed on an outdoor test cell, as described in the following sections.

4.1. Glazed system

The glazed system tested is a double glazed unit made of an 8 mm clear pane of glass, a 12 mm cavity filled with air, and a 6 mm reflective glass pane, facing the outside environment. The optical properties of each glass panes have been characterised through spectrophotometric analysis carried out by means of a Perkin Elmer Lambda 9 UV/VIS/NIR double-monochromator spectrophotometer (Micono, 2006). The measured spectral transmittance and reflectance profiles are reported in Fig. 2. The effective properties for the double glazed system calculated with the software tool WINDOW by LBL, following the relevant international standard procedures (ISO 15099, 2003). The effective direct solar transmittance (with normal incident radiation) τ_e is 0.27; the effective (with beam angle close to 0 deg.) solar reflectance ρ_e is 0.33. The nominal thermal transmittance and the nominal solar factor has also been calculated. The resulting thermal transmittance of the glazed unit is 2.79 W/m^2 K; the nominal solar factor (correspondent to a beam perpendicular to the window plane) is 0.40.

Figure 2

4.2. Test-rig

The south-facing façade of an outdoor test cell (Test Cell A) of the experimental test rig TWINS (Testing Window Innovative System) (Fig. 3) was equipped with a curtain-wall façade hosting the double glazed unit (Serra et al., 2010). The experimental test rig consists of two identical test cells allowing comparative tests to be carried out. The internal sizes of the test cells are 1.6 m wide, 3.6 m long and 2.5 m high. Their walls, floor, and ceiling are made of 48 mm thick sandwich panels, in double painted sheet-steel with expanded

polyurethane (U-value of 0.43 W/(m^2 K)). The test cells are located in Turin (latitude: 45 ° 06 ’ N; longitude: 7 ° 66 ’ E; elevation: 239 m) on the roof of the laboratory of the Department of Energy of the Polytecnic Univeristy, and their south-exposed façades are not shaded from surrounding buildings or vegetation.

The indoor air temperature of both cells is controlled by means of a full air system with a tolerance of ± 1 °C. The temperature set-point adopted during the experimental campaign was 20 °C in winter, 23 °C during the mid seasons, and 26 °C in summer. PT100 termometers are used to control the HVAC of the facility.

The measurement equipment consisted of two pyranometers, two temperature sensors (T-type) for the indoor and outdoor air temperature, three heat flux meters for the monitoring of the heat flux exchanged by each of the three glazed units (the façade hosted three glazed units with the same configuration, see Fig. 3), and six T-type thermocouples (two each glazing) to record the inside and ouside surface temperatures (a quantity not necessary for the application of the method, but recorded for control purpose). The values of the heat flux meters (and on the surface temperatures) presented in the next sections have been calculated as average of the three values for the three identical glazed unit configurations installed in the test cell.

The measurement chain (sensor coupled to the data logger acquisition channel) was preliminarily calibrated and/or verified in the laboratory. The accuracy of the sensors (all of them were either new or with less than 2 years of operation at the beginning of the experimental campaign), after the factory calibration or in-house laboratory verification was: ± 0.3 °C for T-type thermocouples; ± 5% for the heat-flux meters; ± 9% for pyranometers.

Sensors subjected to possible interferences by solar radiation were shielded from solar irradiance based on previous experiences developed in previous measurements of façade systems (Corgnati et al., 2007). In particular: thermocouples for air temperature measurement were shaded by a chromate brass cylinder (length 150 mm, diameter 30 mm) and ventilated by micro-fans located in the upper part of the cylinder; the thermocouples on the glass surface (not necessary to carry out the procedure presented in the method but useful for control purpose) were shaded by a plastic semi-cylinder covered by bright aluminium; the heat flux meters were shaded by a bright aluminium square film attached directly onto the opposite side of the glass where the

sensors were installed (i.e. on the outside pane of the glazing). The measurements were performed with a scan rate of 150 s, and averaged every 15 min.

Figure 3

4.3. Experimental data collection and processing

The experimental data acquisition lasted for over two years, with continuous periods up to several months were interrupted because of maintenance and change in the experimented technologies in Test Cell B. In fact, the measurement on the simple curtain-wall system was carried out in conjunction to experimental activities on mechanically ventilated and naturally/hybrid ventilated double skin facades, installed on the other cell of the TWINS system. Data collected in 15 minute intervals where averaged to obtain hourly data, which are the basis of the procedure adopted in this paper.

The analysis presented in this case study is carried out on a data set made of 3168 sets of hourly data, corresponding to 132 days grouped in continuous periods, almost evenly distributed between the four seasons, which included both clear sky days and cloudy sky days. For the sake of the assessment of the goodness of the proposed method, the total data-set available has been divided into two sub-sets of 76 days each: one is used to determine the in-situ thermal transmittance and solar factor (Data Series 1); the other sub-set is instead used to validate the finding from the first one (Data Series 2), as explained in the next section.

Figure 4

The distribution of the days of the total data-set in two sub-groups have been carried out in order to assure that both the sub-sets are representative of the entire year, and are therefore also comparable with each other. In Fig. 4, the two sub-sets are represented in terms of degree days (*DD*) [°C h] (Fig. 4 a), as defined in Eq. 14, and of daily area specific global solar irradiation of the external vertical, south-exposed plane (G_{24}) [kWh/m^2] (Fig. 4 b), as defined in Eq. 15, calculated based on experimental data with a time-step of 1 h.

$$DD = \int_{06:00}^{+1\ \text{day}} (T_{in} - T_{out})dt = \sum_{i=1}^{24} (T_{in,i} - T_{out,i})\ [^{o}\text{C day}] \quad (14)$$

$$G_{24} = \int_{06:00}^{+1\,\text{day}} E_{out}\,dt = \sum_{i=1}^{24} (E_{out,i})\,[\text{J}] \quad (15)$$

As specified in the description of the method, the in-situ thermal transmittance was assessed only through linear regression on night data. Furthermore, only night data when the measured specific surface heat flux dq was greater than 5 W/m^2 or smaller than -5 W/m^2 were used. The reason for this choice is that the inaccuracy of the heat flux meter sensors become greater the closer the measured heat flux is to 0 W/m^2, and the adoption of such a rule is considered a conservative approach to assure a lower inaccuracy on the assessed values of $\overline{U}$. For a similar reason, the linear regression leading to the evaluation of $\bar{g}$ was calculated using day-time readings when the transmitted solar irradiance E_{in} was greater than 10 W/m^2 – this threshold value being chosen because the inaccuracy of pyranometers are higher in case of very low irradiance. No correction on the readings of the pyranomenter recording the transmitted solar irradiance were carried out to take into account the effect of back-reflected irradiance from the glazing. This choice will be justifiedmore in detail in the Discussion section.

4.4. Evaluation of the in-situ assessment method

The aim of the proposed method is to assess the in-situ performance of a glazed system through the determination of the equivalent thermal transmittance and solar factor. These two values might be relatively far from the nominal thermal transmittance and solar factor, because these depends on boundary conditions set by the international standard procedures, which might be relatively far from those occurring under real operations (this is particularly true for the solar factor). This means that a direct comparison between the measured/calculated nominal U-value and g-value with the correspondent, in-situ $\overline{U}$ and $\bar{g}$ might not allow an assessment of the proposed method to be carried out – i.e. the differences in values between U and $\overline{U}$, and between g and $\bar{g}$ might not be necessarily due to an inaccuracy of the proposed method. For this reason, a different approach to validate the non-calorimetric method needs to be adopted.

A first level of assessment was carried out during the execution of the proposed method through residual analysis. Normalised residuals e_n (Eq. 16, where y is the observed value and $\hat{y}$ is the predicted value) of the dependent variable (i.e. dq when assessing $\overline{U}$ and dq_g when assessing $\bar{g}$) where plotted against the dependent variable to verify random patterns, which are indication of a good fit for of the linear model proposed.

$$e_n = \frac{y - \hat{y}}{y} \quad (16)$$

As a second level of assessment, the capability of the identified $\bar{U}$ and $\bar{g}$ of replicating the (in-situ) thermophysical behaviour of the glazed system has been evaluated by comparing the measured physical quantities constituting the experimental data set Data Series 2 with the correspondent, predicted ones derived by the use of the proposed method on experimental data contained in the Data Series 1 (and making use of the boundary conditions of Data Series 2). Such an assessment process has been carried out comparing the predicted and experimental specific total hourly heat flux entering the indoor environment through the glazing ($dq_{TOT,sim}$ and $dq_{TOT,exp}$ [W/m^2]) and the predicted and experimental specific total daily energy entering the indoor environment ($q_{TOT,sim}$ and $q_{TOT,exp}$ [Wh/m^2]), which is the integral of the hourly heat flux over one day (Eq. 17), i.e. Δt is 24 h.

The simulated values $dq_{TOT,sim}$ and $q_{TOT,sim}$ are calculated, recalling the Eq. 1 and 3, using the boundary conditions E_{out}, T_{out}, and T_{in} available in the dataset Data Series 2 and the in-situ thermal transmittance and solar factor determined through the presented method on experimental quantities in Data Series 1 (Eq. 18, 19).

$$q_{TOT} = \int_{06:00}^{+\ 1\ \text{day}} dq_{TOT}\, dt = \left(\sum_{i=1}^{24} dq_{TOT,} \right) \cdot \Delta t \quad (17)$$

$$dq_{TOT,sim} = \left[E_{out} \cdot \bar{g} \right] - \left[(T_{in} - T_{out}) \cdot \bar{U} \right] \quad (18)$$

$$q_{TOT,sim} = \int_{06:00}^{+1\ \text{day}} dq_{TOT,sim}\, dt = \left[\sum_{i=1}^{24} \left[E_{out,i} \cdot \bar{g} \right] - \left[(T_{in,i} - T_{out,i}) \cdot \bar{U} \right] \right] \cdot \Delta t \quad (19)$$

The experimental values $dq_{TOT,exp}$ and $q_{TOT,exp}$ are instead calculated using the experimental data available in the dataset Data Series 2 according to Eq. 20 and 21.

$$dq_{TOT,\exp} = E_{in} + dq \quad (20)$$

$$q_{TOT,\exp} = \int_{06:00}^{+1\ \text{day}} dq_{TOT,\exp}\, dt = \left[\sum_{i=1}^{24} E_{in,i} + dq_i \right] \cdot \Delta t \quad (21)$$

The comparison between predicted, simulated quantities and experimental ones has then been assessed by means of both qualitative (time profiles) and quantitative indicators. As far as the latter ones are concerned, the Root Square Mean Error, *RSME* ([W/m^2] or [Wh/m^2]) of the predicted $dq_{TOT,sim}$ and $q_{TOT,sim}$, has been

determined, as well as the absolute percentage error $|\varepsilon_{\%}|$ [%], according to according to Eq. 22 and 23, respectively, where *s* indicates the simulated datum ($dq_{TOT,sim}$ or $q_{TOT,sim}$) and *e* refers to the experimental datum ($dq_{TOT,exp}$ or $q_{TOT,exp}$).

$$RSME = \sqrt{n^{-1} \cdot \sum_{i}^{n} \left(\mathrm{s}_i - \mathrm{e}_i\right)^2} \quad (22)$$

$$\left|\varepsilon_{\%}\right|_i = 100 \cdot \left|\mathrm{s}_i - \mathrm{e}_i\right| \cdot \left(\mathrm{e}_i\right)^{-1} \quad (23)$$

5. Results from the case study

5.1. Determination of in-situ thermal transmittance $\bar{U}$ and in-situ solar factor $\bar{g}$

In Fig. 5 a, the linear regression leading to the determination of the equivalent solar transmittance (one value for the entire year) is pictured. Attempts were also made to verify whether three (or four) seasonal values of thermal transmittance might be significant. This is because external boundary conditions might be different in different seasons. The $\bar{U}$ based on all-season regression was found to be 2.1 W/m^2 (because of the accuracy of the method, it makes no sense to use two decimal places), while the same value obtained for each individual season (summer, winter, and mid-season) is in the range 2.0 to 2.3 W/m^2. Because of the proximity of these values (withing the ± 10 % range), and the high value of the coefficient of determination of the linear regression, the year-round value of 2.1 W/m^2 was considered to be accurate enough, and used in the following steps of the procedure for the assessment of the equivalent solar factor $\bar{g}$.

The grafical analysis of the residuals (Fig. 5 b) confirms the good fitness of the model, showing a random distribution of the normalised residual around 0. It is worth highlighting that the closer the specific surface is to heat flux *dq* to 0, the higher the residuals (a common event because of the normalisation process and of the lower accuracy of the heat flux meter close to the 0 value) are. Fig. 5 b shows a slight predominance of positive residuals when moving from negative heat fluxes towards null heat flux, and negative residuals for the few cases when the heat flux was (slightly) positive. This may lead to the suggestion to increase the range of heat flux measurements to be excluded from the linear regression from - 5 W/m^2 < *dq* < + 5 W/m^2 to - 10 W/m^2 <

$dq < +10$ W/m^2, since values in this range are revealed to be potentially affected by (larger) inaccuracy than the others.

The evaluation of the in-situ solar factor has started with the attempt tofind a single value for this metric, regardless of the seasons, resulting in a equivalent solar factor of 0.30. In Fig. 6 a, the scattered plot and linear regression between the total transmitted solar flux dq_g (see Eq. 9) and the impinging solar radiation on the glazing plane E_{out} is reported, while the normalised residual are shown in Fig. 6 b. It is possible to see that, even if the coefficient of determination of the linear regression is satisfactory, there are patterns that are not well described by the linear regression. The residuals are also characterised by relatively high values in correspondance with very low total transmitted solar fluxes (probably due to the combination of the normalisazion process and of the higher uncertainty of the measurements when the total transmitted solar flux is low), while show a satisfactory distribution when the value of dq_g increases.

Figure 5

Figure 6

In order to improve the fitness of the model, and acknowledging the sensible seasonal dependence of effective solar factor, data has therefore been grouped according to the season (winter, summer, and mid-season), and linear regressions carried out for each of these periods. Such an approach has lead to the determination of three different in-situ solar factors, which depend on the season (Fig. 6 c). The adoption of three different values increase the accuracy of estimated metric(s) and allows a better match between experimental data and model(s) to be achieved. The resulting values for the in-situ solar factor(s) are: 0.36 for the winter, 0.32 for the mid-season, and 0.18 for the summer.

In conclusion, it is possible to see that the in-situ thermal trnasmitttance and in-situ solar factor differ substantially from the nominal values of these metrics, calculated according to the standardised procedures (cf nominal values reported in Section 4.1). A throughout explaination for these discrepancies are given in the Discussion section.

5.2. Evaluation of the in-situ assessment method

Singling the residuals analysis carried out during the regression analyses to identify the values for $\overline{U}$ and for $\bar{g}$, a dedicated evaluation of the goodness of the procedure was performed through assessing the capability of the identified values to predict the behaviour of the glazed system.

In Fig. 7 a), the comparison between predicted values (using Eq. 18) and experimental ones (Data Series 2) is shown, assuming a constant value for $\bar{g}$ (i.e. $\bar{g} = 0.30$) for the different seasons. The scattering plot clearly shows an overestimation of the total heat flux crossing the glazing when the experimental, reference value is in the range 0 to 150 W/m^2. This phenomenon can be explained considering the relevant difference between a constant, all-year-round value for $\bar{g}$ and the value for the in-situ solar factor under summer conditions (i.e. 0.18). By using a far greater value for $\bar{g}$ than the one shown in the warm season, the predicted value of the total heat flux is clearly larger than the measured one.

On the contrary, when adopting a variable value for $\bar{g}$ depending on the season in Eq. 18, the correspondence between predicted total heat flux and experimental one is improved (Fig. 7 b). The model still seems to slightly over-estimate dq_{TOT}, especially for lower (below 100 W/m^2) values of the variable, as reaffirmed by a closer look at the residuals. In Fig. 7 b, a higher density of greater residuals is found in the lower range of dq_{TOT}, with normalised residuals in the range – 2 to – 0.5. High values for residuals close to the null value of the heat flux (normalised residuals in the range 0.5 to 2.5) can instead be inferred as results of the normalisation process, and are therefore not really significant in the light of the assessment of the quality of the proposed method. In both case, the RSME is one order of magnitude less than the physical quantities it refers to (ranging from 17.6 to 11.3, while dq_{TOT} spans from around - 50 W/m^2 to around + 300 W/m^2.

Figure 7

The interpretation of the results is confirmed by the analysis of the time-profiles of dq_{TOT}, illustrated in Fig. 8. In the top chart (Fig. 8 a) and middle chart (Fig. 8 b), referring to the winter and the mid-season period, respectively, we see a very good agreement between $dq_{TOT,sim}$ and $dq_{TOT,exp}$ in terms of both time and peak values when using a variable, seasonal solar factor (dark grey solid line), and a lower agreement (though still

acceptable), when using a fix value for $\bar{g}$ regardless of the season (light grey solid line). Conversely, when the analysis moves to the summer (Fig. 8 c), the discrepancy in peak values between predicted and experimental values becomes very large when the seasonal variance of the solar factor is not taken into account (light grey solid line), while it remains in the desired range of accuracy in the case of summer, winter, and mid-season values for the in-situ solar factor. This analysis is important when considering the use of the thermal transmittance and of the solar factor to size the building equipment (i.e. to calculate the design heating and cooling load).

Figure 8

In Fig. 9 (a) and 9 (b), the comparison between predicted and experimental daily total transmitted energy q_{TOT} is shown, for a single value of $\bar{g}$ and for seasonal values of $\bar{g}$, respectively, confirming the findings related to the total transmitted heat flux. It can be easily verified, both qualitatively and quantitatively (through the comparison of the RMSE values), that the adoption of seasonal $\bar{g}$ leads to substantially higher accuracy than the use of just one, constant value for $\bar{g}$ – the RMSE around 230 Wh/m^2 in the latter case, while it is reduced to approximately 55 Wh/m^2 in the case of different values for the solar factor depending on the season.

Figure 9

In Fig. 10, the relative cumulate frequency of the absolute percentage error $|\varepsilon_{\%}|$, both for dq_{tot} and q_{tot}, is plotted. This chart shows that for about 50% of the time, the use of $\overline{U}$ and $\bar{g}$ leads to very accurate prediction of the specific daily total energy that crosses the façade ($|\varepsilon_{\%}| < \pm 5$ %), q_{tot}; for about 90% of the time, the absolute percentage error on q_{tot} is within the range ± 25 %. As far as the total specific heat flow dq_{tot} is concerned, the accuracy of the simplified model that makes use of $\overline{U}$ and $\bar{g}$ is slightly lower, but still acceptable – e.g. the absolute percentage error is within the range ± 25 % for almost 80 % of the time. The discrepancy between the performance in prediction between the daily total energy and the total heat flux can be easily explained considering the relation between the two quantities. The daily total energy is the integral of the total

transmitted heat flux, and therefore errors in predictions (greater or smaller values than the experimental ones) of the latter can be compensated when the total heat flux is summed up to return the daily total energy.

Figure 10

6. Discussion

6.1. In-situ vs. nominal thermal transmittance

In order to compare the measured, in situ thermal transmittance of the glazed unit, and the nominal thermal transmittance, it is useful to carry out an analysis that considers the different elements contributing to the total thermal transmittance metrics, i.e. the thermal conductance of the glazed unit alone and the indoor and outdoor surface heat transfer coefficient of the glazed unit.

The nominal thermal conductance of the glazed unit can be calculated using data on the thermal conductivity of the glass panes (λ = 0.96 W/m K), their thickness (6 mm and 8 mm), and the resistance of the air-layer in the gap, assumed to be equal to 0.155 (m^2 K)/W according to (ISO 6946, 2007). The nominal value for the thermal conductance of the glazed unit alone is thus approximately 5.7 W/m^2 K, and it corresponds to a total nominal thermal transmittance of 2.9 W/m^2 K – calculated with values for internal and external surface resistance according to (ISO 6946, 2007).

Under the assumption of steady state, the thermal conductance of the glazed unit alone can be obtained through linear regression between difference between the indoor and outdoor surface temperature of the glazed unit, and the area specific heat flow measured at the inside facing surface of the glazed system. In Fig. 11 (a), the scattered plot of surface heat flux vs. surface temperature difference is shown, for the three different periods, and for the three glazed units measured (see Fig. 3). In Table 1, the nominal and experimental thermal conductance of the three glazing units are reported.

Figure 11

Table 1

It is possible to see that the in-situ thermal conductance of the glazed unit (and therefore its thermal resistance) depends both on the exact position of the glazed unit in the room (different height) and to a greater extent on the season. In winter, the thermal resistance of the glazing unit alone is comparatively higher than in summer (up to more than 20% higher in the cold season than in the warm season). This behaviour cane, to a certain extent, be explained when considering the non-constant behaviour of the air-gap, whose heat transfer mechanisms depend on the average temperature field. In Fig. 11 b, the frequency of the average (calculated from experimental data) temperature of the air-gap is reported, for different classes. In the winter, the estimated (as average temperature between the recorded surface temperature values of the inside and outside glass pane) values for the temperature in the air-gap are more than 10 °C lower than in the summer (Tab. 1).

The linear regression approach adopted to determine the in-situ thermal transmittance, and the in-situ thermal conductance of the glazed unit(s), can be applied to determine the surface heat transfer coefficients also. Such an analysis, carried out on the case study and not fully reported here for the sake of brevity, shows that the experimental indoor surface heat transfer coefficient has a rather stable value in the range 4 to 5 $W/m^2 K$ – and more in details, a very consistent values around 4.5 $W/m^2 K$ in winter and in mid-season, and a slightly larger range of values in summer. Such a range of values is significantly lower than the value suggested in the relevant technical standards (EN 673, 2011; ISO 6946, 2007; ISO 15099, 2003), which is in the range 7.7 to 8 $W/m^2 K$ – and that correspondents to an indoor surface resistance of 0.13 $(m^2 K)/W$. There are discrepancies between standardised values and on-site values, especially because of the contribution of the convective heat exchange, is a well-known problem (e.g. (Emmel et al., 2007; Hoffmann and Geissler, 2017; Palyvos, 2008; Tejedor et al., 2017)).

With regards to the outdoor surface heat transfer coefficient, a proper linear regression analysis does not lead to a robust, constant value (or value ranges). This is because of the intrinsicly higher complexity of this quantity (when compared to the one for the indoor surface), as well as to the fact that to properly assess it, a heat flux meter installed on the outside-facing surface of the glazing (sensor 6 in Fig. 1) is required. However,

an evaluation of the external surface heat transfer coefficient can still be done under some assumptions, not presented herewith for the sake of brevity, and this lead to values in the range of 5 to 15 W/m^{2}K for almost 99%, 50%, and 80% of the time, for the winter, mid-season, and summer season, respectively. These values are approximately half (or even less than half) of the one used in the standardized *U* calculation, which is equal to 25 W/m^{2}K. The reason for such an observed phenomenon can be explained considering that the value in the technical standard is computed with a wind speed of 4 m/s (a quite high speed) and a lower (compared to the standardised calculation) radiative heat exchange with the surroundings.

In Table 2, the experimentally assessed and the nominal values of the internal and external surface heat transfer coefficients, are reported for the different seasons. The discrepancy between the experimental (in-situ) values of these coefficients and the values used in the nominal thermal transmittance calculation, together with the experimental measurement error, can well explain the difference between the standardised U and in-situ $\overline{U}$.

Table 2

The in-depth analysis of the surface heat transfer coefficient, and on the thermal conductance of the glazed unit alone has highlighted, how different boundary conditions in each seasons leads to the determination of seasonal values for $\overline{U}$. However, in section 5, just one yearly value for the in-situ equivalent thermal transmittance has been used. In Fig. 12, a comparison between predicted and experimental values for this quantity is presented, where Fig. 12 a) (already shown in Fig. 7 b) shows the predicted values obtained using one annual value for the in-situ thermal transmittance (and three seasonal values for the in-situ solar factor), while Fig. 12 b shows the predicted values obtained using three seasonal values for the in-situ thermal transmittance (and three seasonal values for the in-situ solar factor). The results are almost identical, and the good performance of the single, annual value for the in-situ thermal transmittance have been already proved by comparing the predicted and experimental time profiles also in a qualitative way (see Fig. 9).

Figure 12

6.2. In-situ vs nominal solar factor

While the use of an annual value for equivalent thermal transmittance seems to be an acceptable solution, the case study has proved the need to characterise (and use in calculations) seasonal values for the in-situ solar factor (see Fig. 6 c; Fig 7 a-b). The main reason for this is that the nominal calculation of the solar factor makes use of standardised boundary conditions (i.e. surface heat transfer coefficient, *cf* section 6.1) that are far away from those occurring under real operations (due to the solar height and solar irradiance incident angle), since the nominal standardised calculation is performed using an angle between the beam and the normal to the glass pane surface close to zero.

In Fig. 13 a, the frequency distribution of angle between the solar radiation beam and the normal to the glazing surface (south-facing vertical glazing) is shown, for different seasons of the year in Torino (Italy). It appears clearly that not only are the conditions used for the calculation of the solar factor never met in this real application (the incident angle is never in the range 0 to 20 deg.), but how different seasons present the very different geometry of the solar radiation: while in winter more than 80% of the time the incident angle is in the range 20 to 60 deg., in summer more than 90% of the values lies in the range 60 to 90 deg. In Fig. 13 b) the solar properties for the glazed unit used in the case study are shown as a function of the incident angle, highlighting how the glazed unit performs in very different ways depending on the incident angle of the solar radiation. The combination of these two phenomena are the main reasons for the observed disagreement between the nominal and the in-situ solar factor.

Figure 13

6.3. Influence of diffuse indoor solar irradiance

Under normal operative conditions (i.e. if no additional provision is taken for the purpose of the measurement), a glazed unit interacts with both the solar irradiance acting on the outdoor surface of the façade, and with the (in almost the totality of the cases) diffuse solar irradiance in the indoor environment resulting from reflection of the transmitted solar irradiance through the glazing. The relevance of such a phenomenon on the measurement procedure varies depending on a series of materials' and geometrical/spatial properties of the

combined system glazing-room. Furthermore, any additional artificial lighting in the indoor environment is also a source of electromagnetic radiation in the spectrum measured by the pyranometers (and thus included in the procedure to assess the in-situ metrics).

In the case study illustrated in Section 5, the influence of the indoor diffuse solar irradiance on the measurement is quite large, because of the features of the test cell's indoor surfaces and of the geometry of the cell, compared to a conventional room.

As far as the indoor surfaces are concerned, though experimental data on the (average) solar reflection coefficient of the test cell are not available, it is reasonable, based on the experience of the authors, to assume a (conservative) estimation for the average value for the whole surface in the range of $\rho_{e,op} = 0.6 \div 0.7$. When it comes to the ratio between the glazed area (of the façade) A_g [m^2] and the opaque surfaces (of the test cell) A_{op} [m^2], this is also a quite "unfavourable" condition, and is in the range of 12% – for reference purpose, a conventional room with dimensions 4 m x 4 m x and 3 m (hight), equipped with 2 windows with a glazed surface of 1.5 m^2 each, presents a glazed to opaque surface ratio of less than 4%.

Given the area-specific directly transmitted solar radiation through the glazing E_{in}, the average diffuse solar irradiance E_{diff} [W] can be approximated by the product of E_{in} , the average solar reflection coefficient of the opaque surfaces of the room ρ_e, and the glased area A_g (Eq. 24) This obtained quantity can be then evenly distributed over the total indoor surfaces (A_g plus A_{op}), in order to calculate the average diffuse irradiance acting on the indoor surfaces[4] (Eq. 25). By multiplying this value and the (indoor side) solar reflection coefficient of the glazed unit ($\rho_{e,ind}$), the diffuse solar irradiance re-reflected (first-reflection) by the glazed unit towards the indoor space $E_{ind,diff,r}$ can be estimated (Eq. 26). This quantity, summed to the direct solar irradiance τ_e is the real physical quantity read by the indoor-installed pyranometer facing the glazed unit (sensor 3 in Fig. 1).

$$E_{diff} = E_{in} \cdot A_g \cdot \rho_{e,op} \quad (24)$$

$$E_{ind,diff} = \frac{E_{diff}}{A_g + A_{op}} \quad (25)$$

[4] When one pyranometer is installed near the glazed unit and faces towards the inside (sensor 9 in Fig 1), this quantity is directly measured.

$$E_{ind,diff,r} = E_{ind,diff} \cdot \rho_{e,ind} \qquad (26)$$

In the case study presented in this paper, which is a worse-case scenario of measurements in real buildings, $E_{ind,diff,r}$ can be estimated to be lower than 2 % of the value of directly transmitted solar irradiance E_{in}. This means that the value measured by the pyranometer (sensor 3 in Fig. 1) can be well approximated to the directly transmitted solar irradiance E_{in}, provided that no additional sources such as lamps of electromagnetic radiation in the range of the solar spectrum are active during the measurement.

In summary, the reading of the directly transmitted solar irradiance, used to calculate the in-situ solar factor, can be carried out with a suitable accuracy using just on pyranometer installed near the inside surface of the glazing. However, when this method is applied to buildings that are occupied and with lighting on, the use of an additional sensor (sensor 9 in Fig. 1) is recommended to measure the diffuse irradiance acting on the glazing.

7. Conclusions

Synthetic metrics (such as U-value and g-value) are widely adopted in present-day design and assessment of energy performance of building. These metrics are calculated using standardised procedures, with the aim of allowing comparison between alternative solutions to be carried out, but assessed in real buildings, these metrics can be relatively far from the nominal values. The reason for such a behaviour is due to the boundary conditions selected in the standardised procedures, which are often correspondent to a "worse-case" scenario. An in-depth analysis of the causes of the discrepancy have been presented, and demonstrated how the surface heat transfer coefficient and the geometry of the solar-to-surface relationship are the two main causes of the discrepancy.

In the paper, the assessment of a simple non-calorimetric method to characterise the in-situ thermal transmittance and solar factor has been presented, and through an application on a case study, the effectiveness of the proposed procedure demonstrated. With a relatively cheap set of sensors and data acquisition system (in the range of EUR 2000 to EUR 3000) and relatively short acquisition times (in the range on one to two weeks each season), the equivalent metrics under real boundary conditions can be estimated with a sufficient degree of accuracy (estimated to be in the range of ± 10 % to 15 % for the two metrics). The assessed quantities have been proved to be reliable in the replication of the thermophysical behaviour of the glazed system, showing that

the daily energy crossing the façade can be estimated for about 90% of the time with an error lower than ± 25 %, and for 50% of the time with an error that is lower than 5 %. Whether these errors (which are anyway very low) are due to the accuracy of the procedure (which is not free from assumption about steady state condition and associated use of simplified heat transfer models) or to the meaningfulness of these performance metrics (the thermal transmittance and the solar factor) is a question that remains open.

Acknowledgments

The authors gratefully acknowledge the contributions of all the people who took part to the experimental campaign on the glazing system presented in the paper, i.e. Silvano Caon, Carlo Micono, Riccardo Issoglio, Marco Perino, Fabio Zanghirella, carried out in the framework of the *PRIN 2005-2007 "Responsive by Renewable - RES2"* research project financed by the Italian Ministry of University and Research. The experimental data post-processing, the evaluation of the methodology, and the writing of this paper has been carried out in the framework of the ENERGIX research project "SkinTech" (255252) and FRINATEK research project *"ReInVent windows"* (262198), both founded by the Research Council of Norway and by the following industrial partners: SINTEF, Saint-Gobain Byggevarer, Nordan, Schüco-Norge (for SkinTech); SINTEF and SAPA Building Systems (for ReInVent windows).

References

Bianco, L., Cascone, Y., Goia, F., Perino, M., Serra, V., 2017a. Responsive glazing systems: Characterisation methods and winter performance. Sol. Energy 155, 372–387. https://doi.org/10.1016/j.solener.2017.06.029

Bianco, L., Cascone, Y., Goia, F., Perino, M., Serra, V., 2017b. Responsive glazing systems: Characterisation methods, summer performance and implications on thermal comfort. Sol. Energy 158, 819–836. https://doi.org/10.1016/j.solener.2017.09.050

Bianco, L., Goia, F., Serra, V., 2013. Energy performance assessment of advanced glazed façades in office buildings, in: Proceedings of CLIMA 2013. Presented at the The 11th REHVA World Congress & 8th International Conference on IAQVEC, Prague, pp. 1–10.

Bianco, L., Goia, F., Serra, V., Zinzi, M., 2015. Thermal and Optical Properties of a Thermotropic Glass Pane: Laboratory and In-Field Characterization. Energy Procedia 78, 116–121. https://doi.org/10.1016/j.egypro.2015.11.124

Corgnati, S.P., Perino, M., Serra, V., 2007. Experimental assessment of the performance of an active transparent façade during actual operating conditions. Sol. Energy 81, 993–1013. https://doi.org/10.1016/j.solener.2006.12.004

Emmel, M.G., Abadie, M.O., Mendes, N., 2007. New external convective heat transfer coefficient correlations for isolated low-rise buildings. Energy Build. 39, 335–342. https://doi.org/10.1016/j.enbuild.2006.08.001

EN 410, 2011. Glass in building - Determination of luminous and solar characteristics of glazing.

EN 673, 2011. Glass in building - Determination of thermal transmittance (U value). Calculation method.

EN 674, 2011. Glass in building - Determination of thermal transmittance (U value). Guarded hot plate method.

EN 675, 2011. Glass in building - Determination of thermal transmittance (U value) - Heat flow meter method.

Favoino, F., Goia, F., Perino, M., Serra, V., 2016. Experimental analysis of the energy performance of an ACTive, RESponsive and Solar (ACTRESS) façade module. Sol. Energy 133, 226–248. https://doi.org/10.1016/j.solener.2016.03.044

Goia, F., Bianco, L., Perino, M., Serra, V., 2014a. Energy Performance Assessment of and Advanced Integrated Façade through Experimental Data Analysis. Energy Procedia 48, 1262–1271. https://doi.org/10.1016/j.egypro.2014.02.143

Goia, F., Perino, M., Serra, V., 2014b. Experimental analysis of the energy performance of a full-scale PCM glazing prototype. Sol. Energy 100, 217–233. https://doi.org/10.1016/j.solener.2013.12.002

Hoffmann, C., Geissler, A., 2017. The prebound-effect in detail: real indoor temperatures in basements and measured versus calculated U-values. Energy Proceida 122, 32–37. https://doi.org/10.1016/j.egypro.2017.07.301

Hukseflux, 2016. User Manual SR03 - Fast response second class pyranometer.

Hutcheson, G.D., 1999. Chapter 3 - Ordinary Least-Squares Regression, in: The Multivariate Social Scientist. Sage.

ISO 6946, 2007. Building components and building elements - Thermal resistance and thermal transmittance - Calculation method.

ISO 8301, 1991. Thermal insulation - Determination of steady-state thermal resistance and related properties - Heat flow meter apparatus.

ISO 8302, 1991. Thermal insulation - Determination of steady-state thermal resistance and related properties - Guarded hot plate apparatus.

ISO 8990, 1994. Thermal insulation - Determination of steady-state thermal transmission properties - Calibrated and guarded hot box.

ISO 9050, 2003. Glass in building - Determination of light transmittance, solar direct transmittance, total solar energy transmittance, ultraviolet transmittance and related glazing factors.

ISO 9060, 1990. Solar energy - Specification and classification of instruments for measuring hemispherical solar and direct solar radiation.

ISO 9869-1, 2014. Thermal insulation - Building elements - In-situ measurement of thermal resistance and thermal transmittance - Part 1: Heat flow meter method.

ISO 10077, 2017. Thermal performance of windows, doors and shutters - Calculation of thermal transmittance.

ISO 10291, 1994. Glass in building - Determination of steady-state U values (thermal transmittance) of multiple glazing - Guarded hot plate method.

ISO 10292, 1994. Glass in building - Calculation of steady-state U values (thermal transmittance) of multiple glazing.

ISO 10293, 1997. Glass in building - Determination of steady-state U values (thermal transmittance) of multiple glazing - Heat flow meter method.

ISO 12567-1, 2010. Thermal performance of windows and doors -Determination of thermal transmittance by the hot-box method - Part 1: Complete windows and doors.

ISO 13790, 2008. Energy performance of buildings - Calculation of energy use for space heating and cooling.

ISO 15099, 2003. Thermal performance of windows, doors and shading devices — Detailed calculations.

Kuhn, T.E., 2014. Calorimetric determination of the solar heat gain coefficient g with steady-state laboratory measurements. Energy Build. 84, 388–402. https://doi.org/10.1016/j.enbuild.2014.08.021 0378-7788

Micono, C., 2006. Facciate trasparenti attive: analisi prestazionali attraverso misure in test cells (Transparent active facades: performance analysis through test cells measurements) (Doctoral Thesis). Polytecnic University of Turin, Torino.

NFRC 201, 2017. Procedure for Interim Standard Test Method for Measuring Solar Heat Gain Coefficient of Fenestration Systems Using Calorimetry Hot Box Methods.

Pagliano, L., Cattarin, G., Causone, F., Kindinis, A., 2017. Improved methods for the calorimetric determination of the solar factor in outdoor test cell facilities. Energy Build. 153, 513–524. https://doi.org/10.1016/j.enbuild.2017.07.028

Palyvos, J.A., 2008. A survey of wind convection coefficient correlations for building envelope energy systems' modeling. Appl. Therm. Envineering 28, 801–808. https://doi.org/10.1016/j.applthermaleng.2007.12.005

Serra, V., Zanghirella, F., Perino, M., 2010. Experimental evaluation of a climate façade: Energy efficiency and thermal comfort performance. Energy Build. 42, 50–62. https://doi.org/10.1016/j.enbuild.2009.07.010

Tejedor, B., Casals, M., Gangolells, M., Roca, X., 2017. Quantitative internal infrared thermography for determining in-situ thermal behaviour of façades. Energy Build. 151, 187–197. https://doi.org/10.1016/j.enbuild.2017.06.040

List of Tables with Captions

Table 1. Nominal and experimental thermal conductance of the glazed units alone (without the surface thermal resistance), in different seasons.

	Λ [W/m^2 K]			
	Nominal	Lower glazed unit	Middle glazed unit	Upper glazed unit
Winter		5.9	6.0	6.2
Mid-season	5.7	6.3	6.2	6.6
Summer		7.3	7.2	7.1

Table 2. Nominal and experimental internal and external surface heat transfer coefficients (average values for the three glazed units) in different seasons.

	h_i [W/m^2 K]		h_e [W/m^2 K]	
	Nominal	Experimental	Nominal	Experimental
Winter		4.5		5 ÷ 10 (90% of the time)
Mid-season	8	4.5	25	5 ÷ 25 (50% of the time)
Summer		4 ÷ 5		5 ÷ 15 (80% of the time)

List of Figures Captions

Figure 1. *Schematic representation of the energy flows, correspondent nomenclature, and sensors. 1: heat flux meter measuring heat flux exchanged at the indoor interface of the glazing with the indoor environment (dq); 2: temperature sensor measuring indoor air temperature (T_{in}); 3: pyranometer measuring global (on vertical plane) transmitted solar irradiance (I_{in}); 4: temperature sensor measuring outdoor air temperature (T_{out}); 5: pyranometer measuring global (on vertical plane) impinging solar irradiance (I_{out}); 6 (optional) heat flux meter measuring heat flux exchanged at the outside interface of the glazing with the outdoor environment; 7: (optional) temperature sensor measuring outside pane surface temperature; 8: (optional) temperature sensor measuring inside pane surface temperature; 9: (optional) pyranometer measuring diffuse (on vertical plane) solar irradiance in the indoor environment.*

Figure 2. *Measured spectral solar transmittance and spectral solar reflectance for the clear glass pane (a) and for the reflective (b) glass pane.*

Figure 3. *View from the outside and from the inside of the two Test Cells, with the Test Cell equipped with the curtain-wall system and the double glazed unit in the front. Temperature and heat flux meter sensors have been suitably shielded from the influence of solar irradiance.*

Figure 4*. Degree-days (a) and daily global solar irradiance on the window plane (b) for the different sub-sets – Data Series 1 is for the assessment of in-situ thermal transmittance and solar factor, Data Series 2 is for the assessment of the method presented in the paper.*

Figure 5. *(a) Linear regression leading to the determination of the in-situ thermal transmittance $\bar{U}$; (b) scattered plot of normalised residuals of the surface heat flux vs. measured surface hear flux.*

Figure 6. *(a) Linear regression leading to the determination of the yearly value in-situ solar factor, $\bar{g}$; (b) scattered plot of normalised residuals of the total transmitted solar flux (see Eq. 9) vs. measured total transmitted solar flux, for the case of one yearly value for $\bar{g}$; (c) linear regressions leading to the determination of three (seasonal) values for the in-situ solar factor $\bar{g}$.*

Figure 7. *Comparison between predicted (through $\bar{U}$ and $\bar{g}$) and experimental total transmitted heat flux. (a) Simulated dq_{TOT} values are obtained with a constant value of $\bar{g} = 0.3$ (b) simulated dq_{TOT} values are obtained using three, seasonal values for $\bar{g}$; (c) normalised residual scattering plot in the case of $dq_{TOT,sim}$ values obtained using three, seasonal values for $\bar{g}$.*

Figure 8. *Comparison between time-profiles of predicted and of the experimental total transmitted heat flux, in case of one constant value for $\bar{g}$ (light grey solid line) and three seasonal values for $\bar{g}$ (dark grey solid line), in different periods of the year. (a) Winter; (b) Mid-season; (c) Summer.*

Figure 9. *Comparison between predicted (through $\bar{U}$ and $\bar{g}$) total daily energy entering the indoor environment. (a) Simulated $q_{TOT,sim}$ obtained with a constant value $\bar{g} = 0.3$; (b) simulated $q_{TOT,sim}$ obtained with three, seasonal values for $\bar{g}$.*

Figure 10. *Relative cumulated frequency of the percentage error $|\varepsilon\%|$ [%] of the predicted specific hourly total heat flux and of the specific daily total energy – in both cases three seasonal values for $\bar{g}$ are used.*

Figure 11. *(a) Linear regression leading to the determination of the in-situ thermal conductance of the three glazed units with identical configurations, in different seasons; (b) distribution of (calculated) air-gap temperature in different season.*

Figure 12. *Comparison between predicted (through $\bar{U}$ and $\bar{g}$) total transmitted heat flux. (a) Simulated $dq_{TOT,sim}$ obtained with a constant, annual value for $\bar{U}$; (b) simulated $dq_{TOT,sim}$ obtained with three, seasonal values for $\bar{U}$. In both cases, three seasonal values for $\bar{g}$ were used.*

Figure 13. *a) Frequency distribution of angle between the solar radiation beam and the normal to the glazing surface (south-facing vertical glazing), for different seasons of the year in Torino (Italy). b) Solar transmittance, reflectance, and absorptance for the double glazed unit used in the case study, as a function of the incident angle of the electromagnetic radiation, as calculated by WINDOW based on spectrophotometric data.*

Figure 1

Click here to download high resolution image

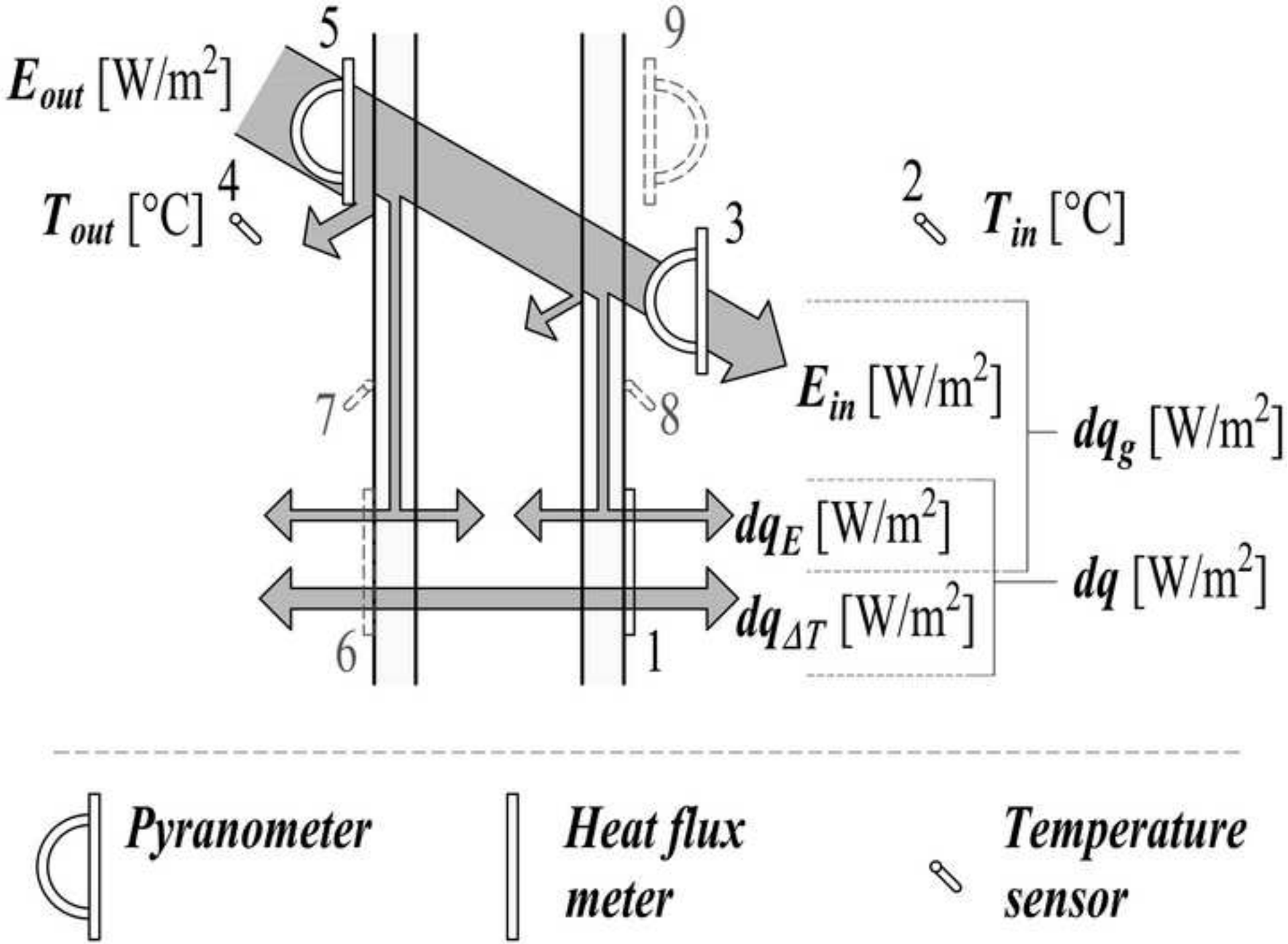

Figure 2

Click here to download high resolution image

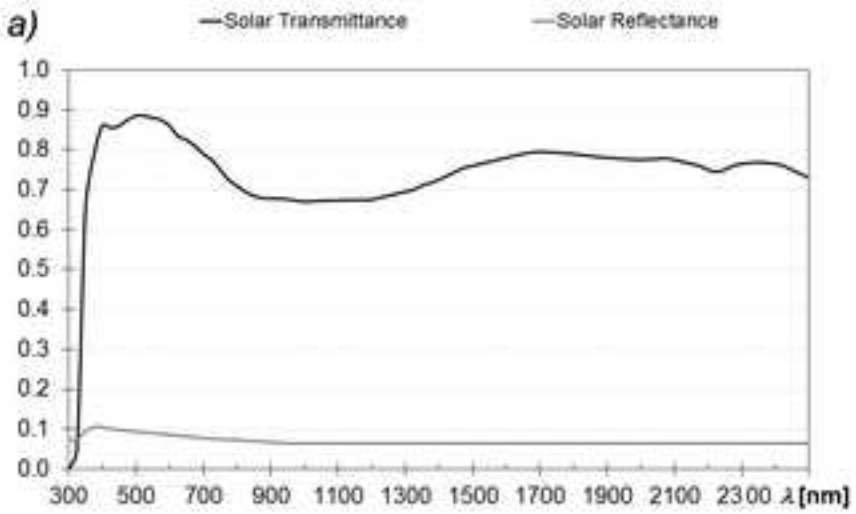

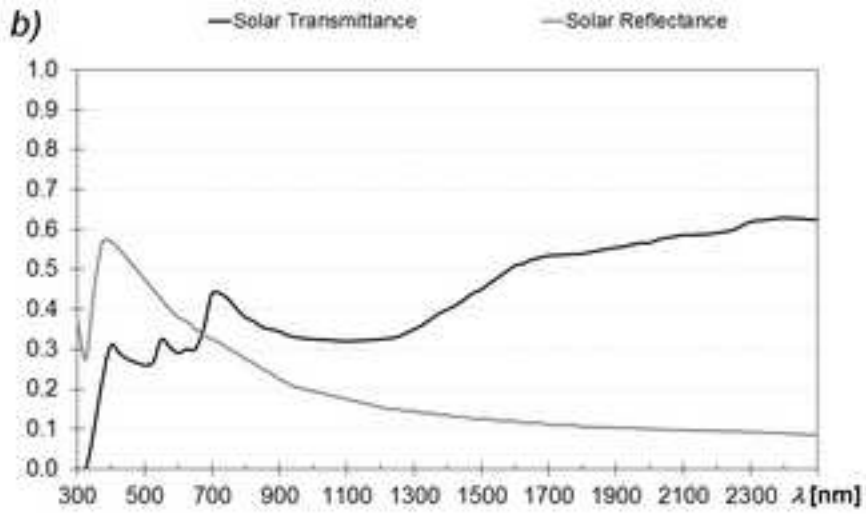

Figure 3

Click here to download high resolution image

Figure 4

Click here to download high resolution image

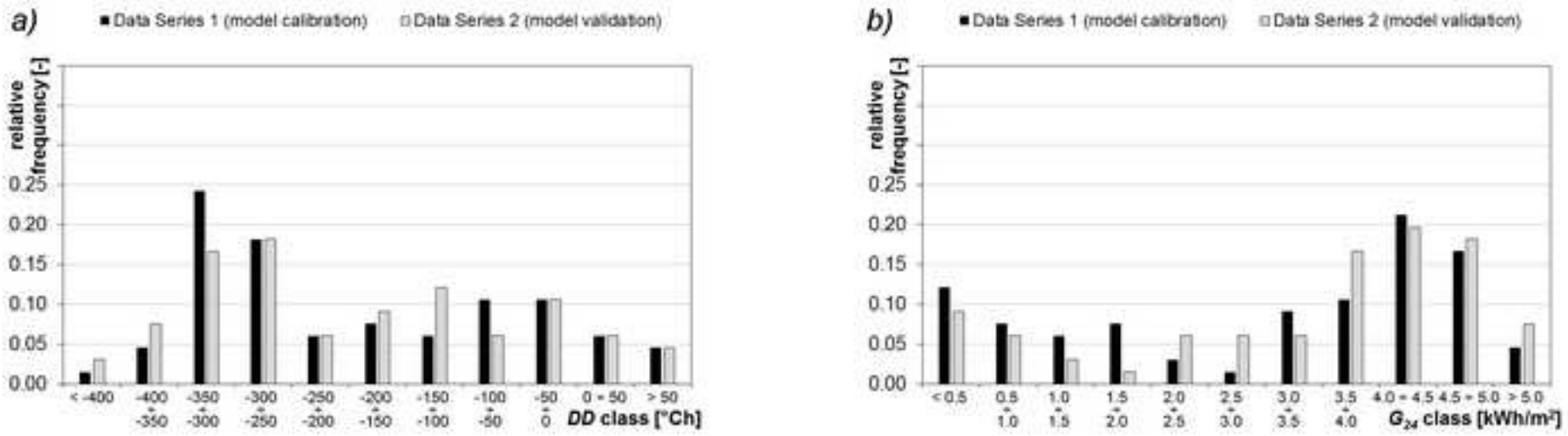

Figure 5

Click here to download high resolution image

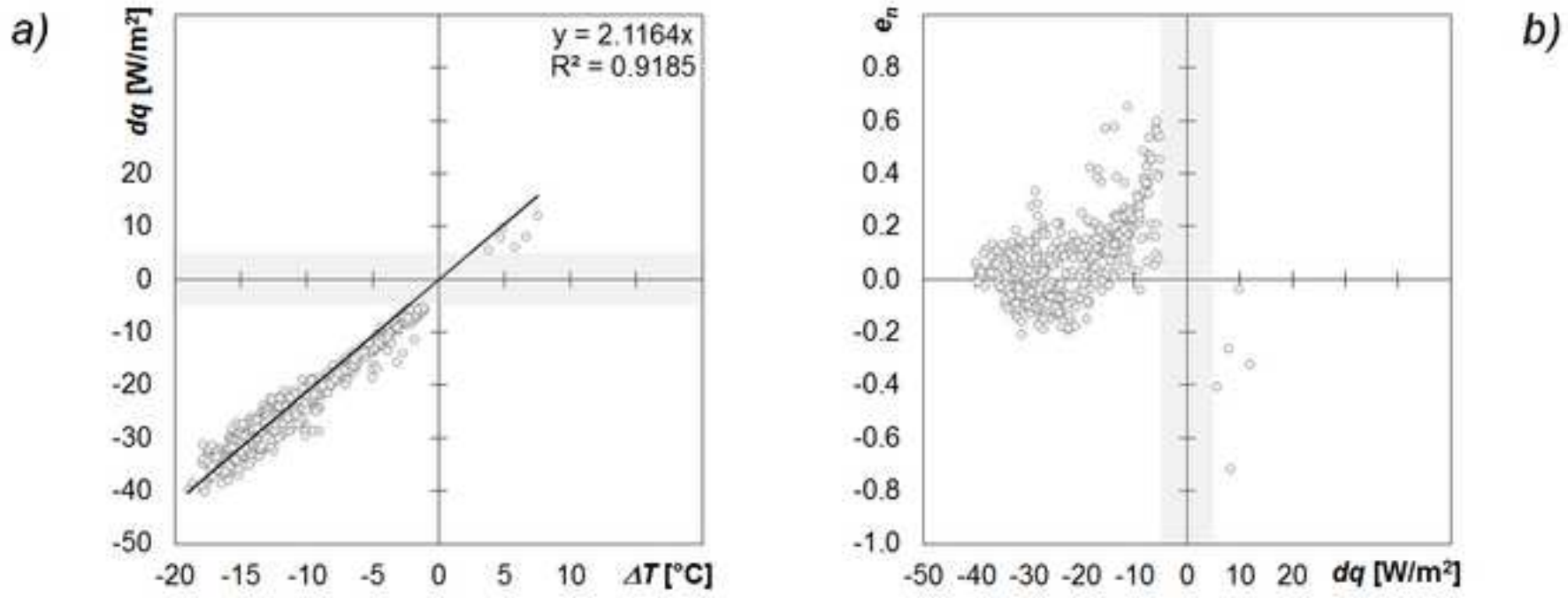

Figure 6

Click here to download high resolution image

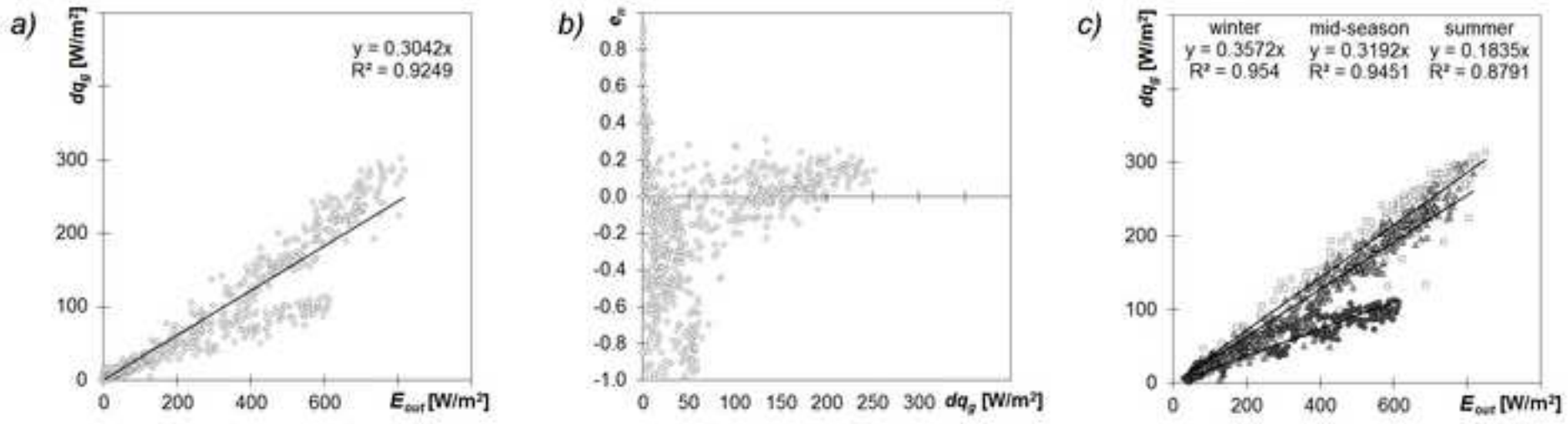

Figure 7

Click here to download high resolution image

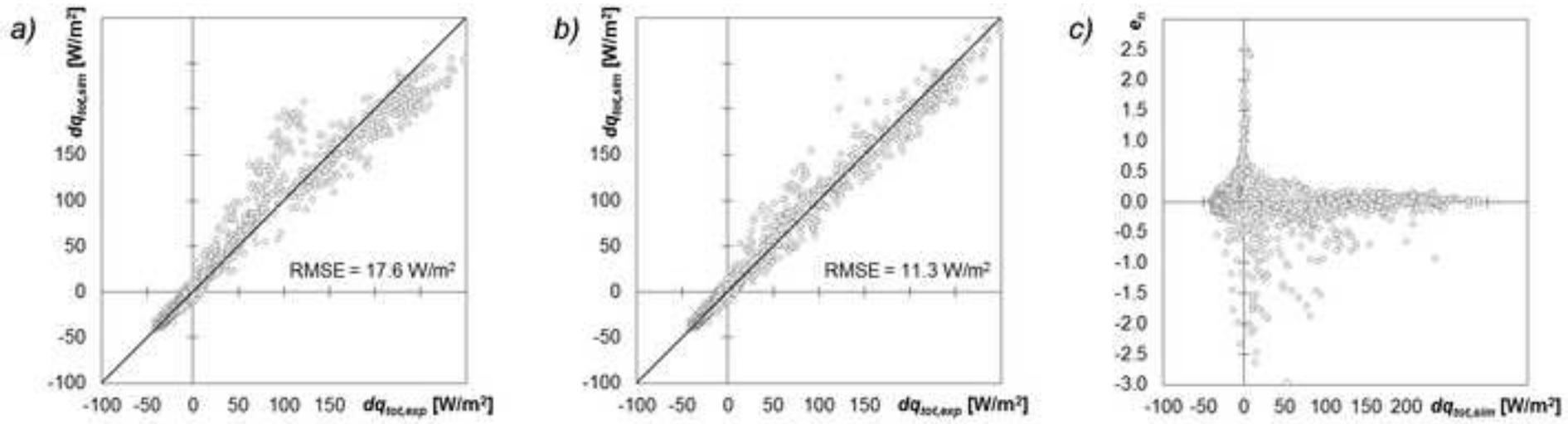

Figure 8

Click here to download high resolution image

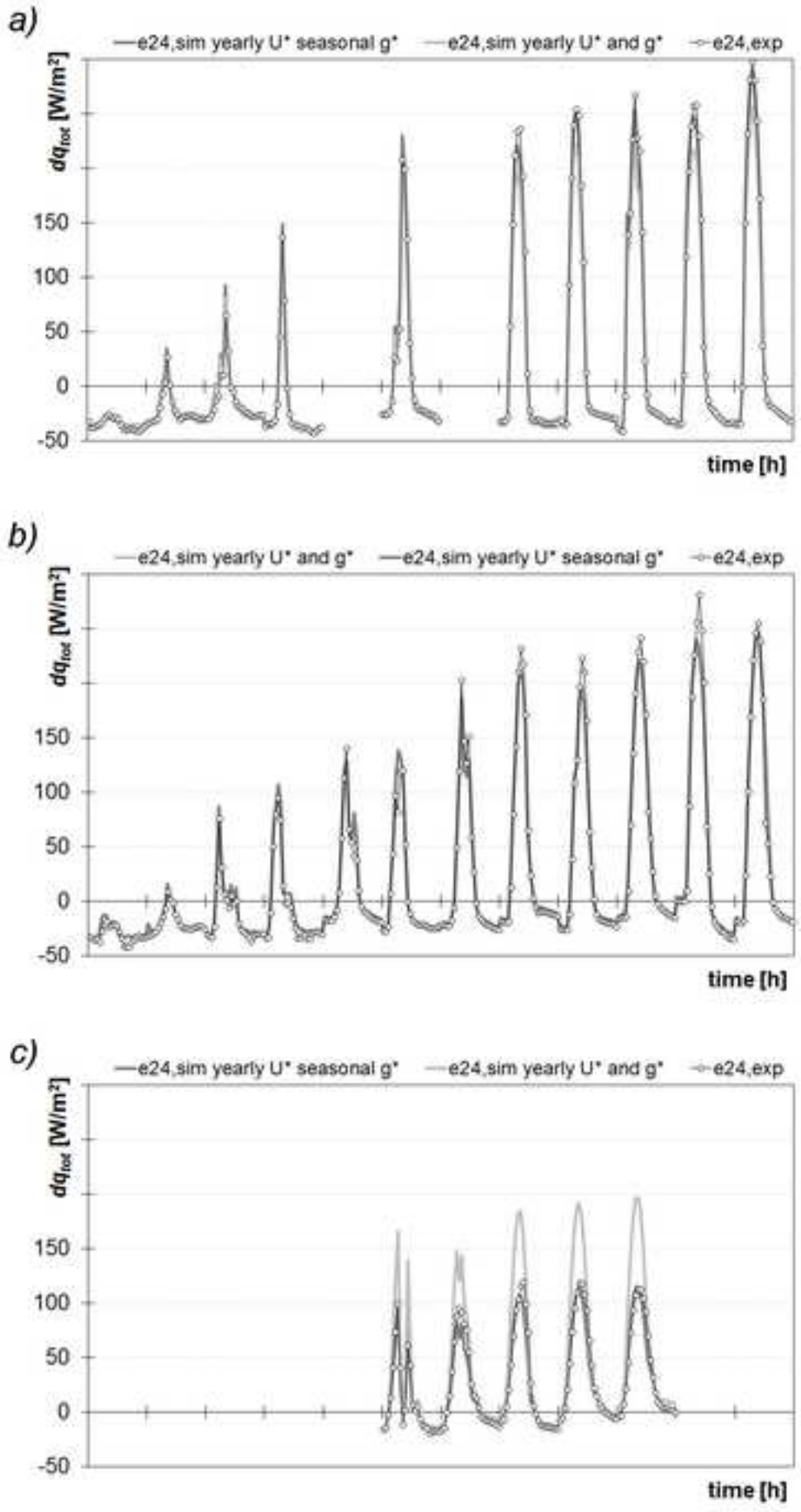

Figure 9

Click here to download high resolution image

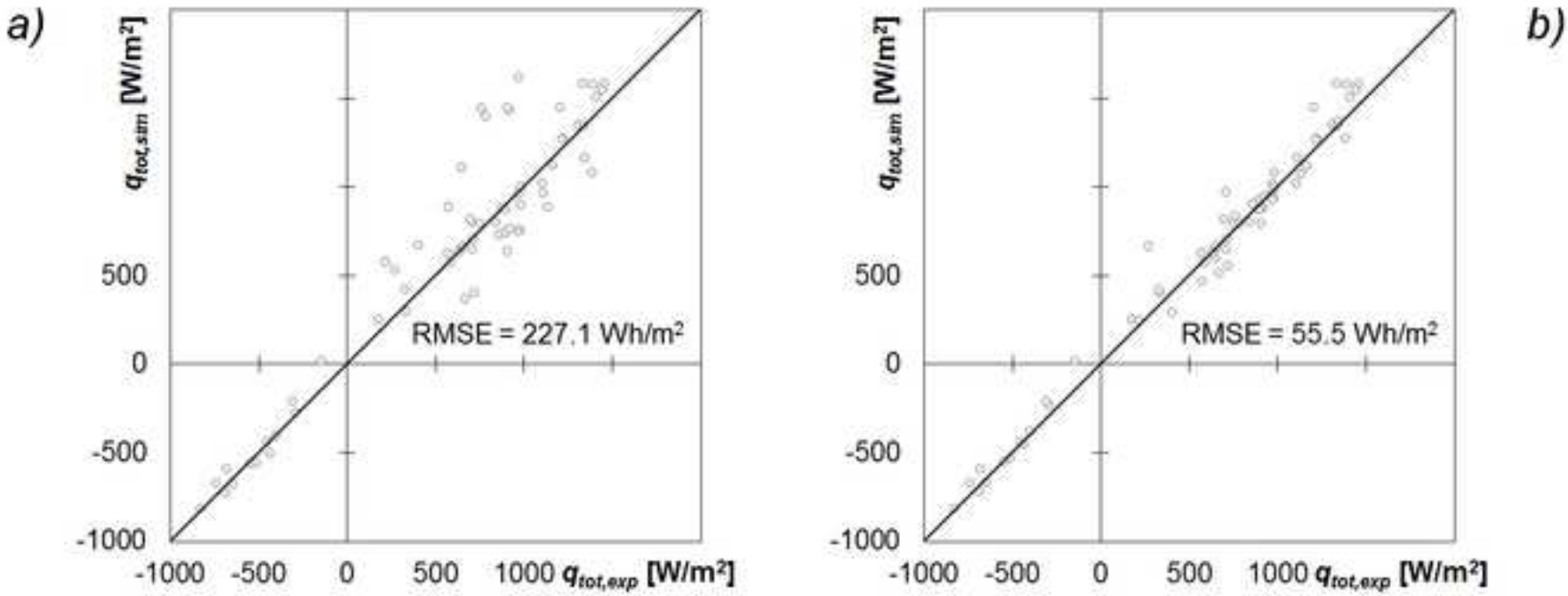

Figure 10

Click here to download high resolution image

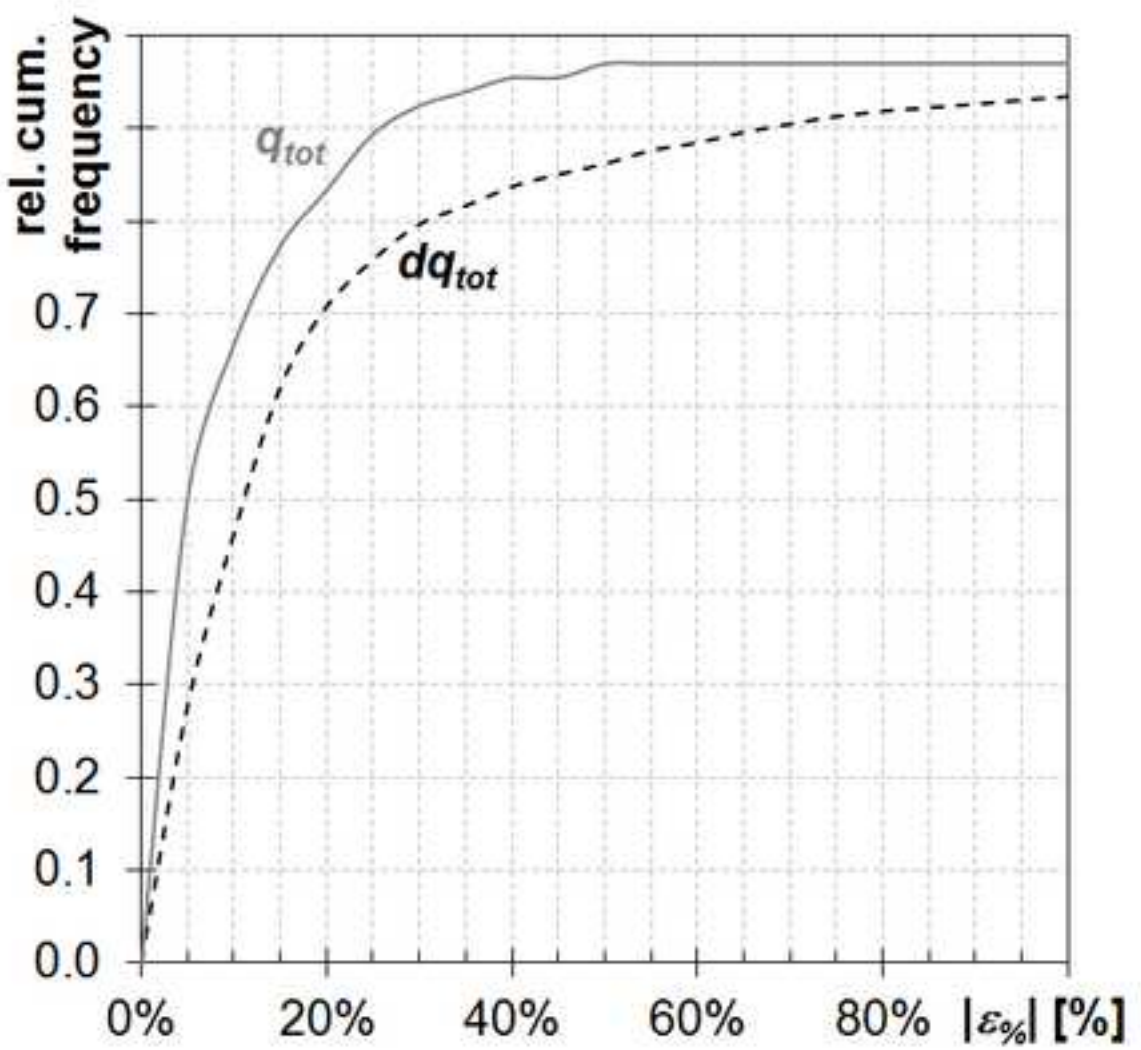

Figure 11
Click here to download high resolution image

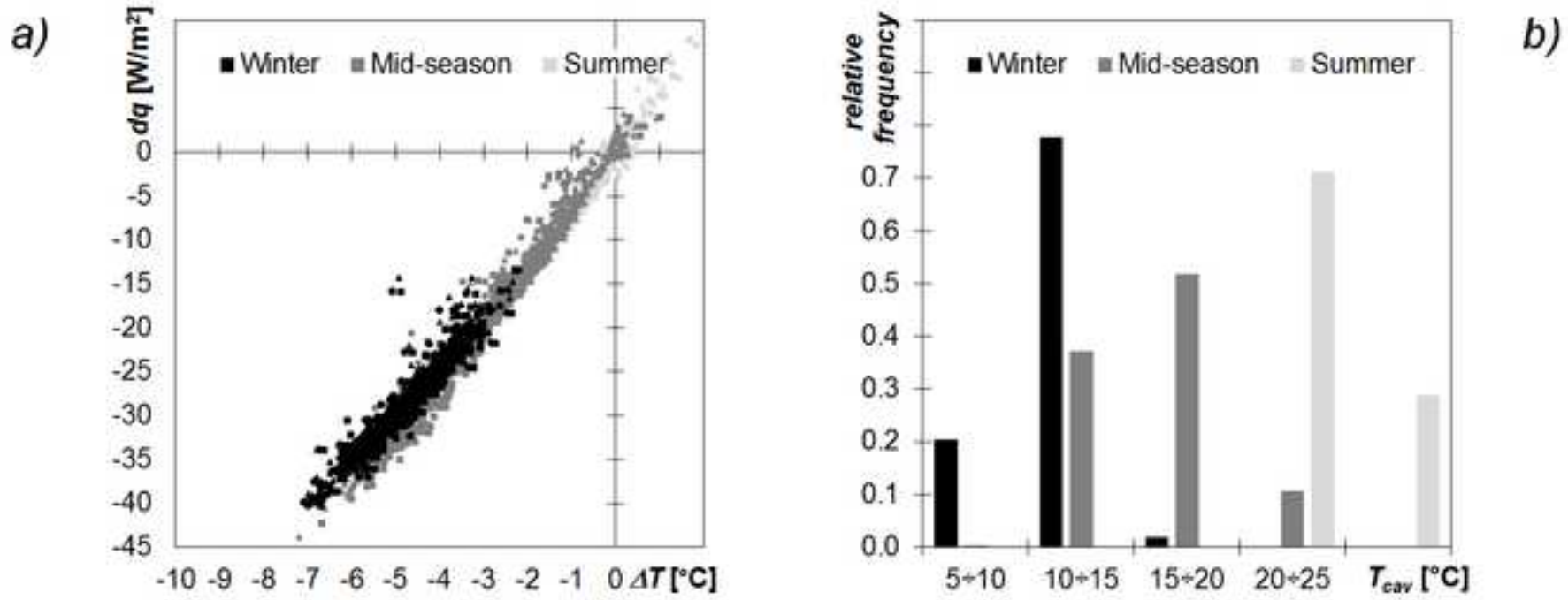

Figure 12

Click here to download high resolution image

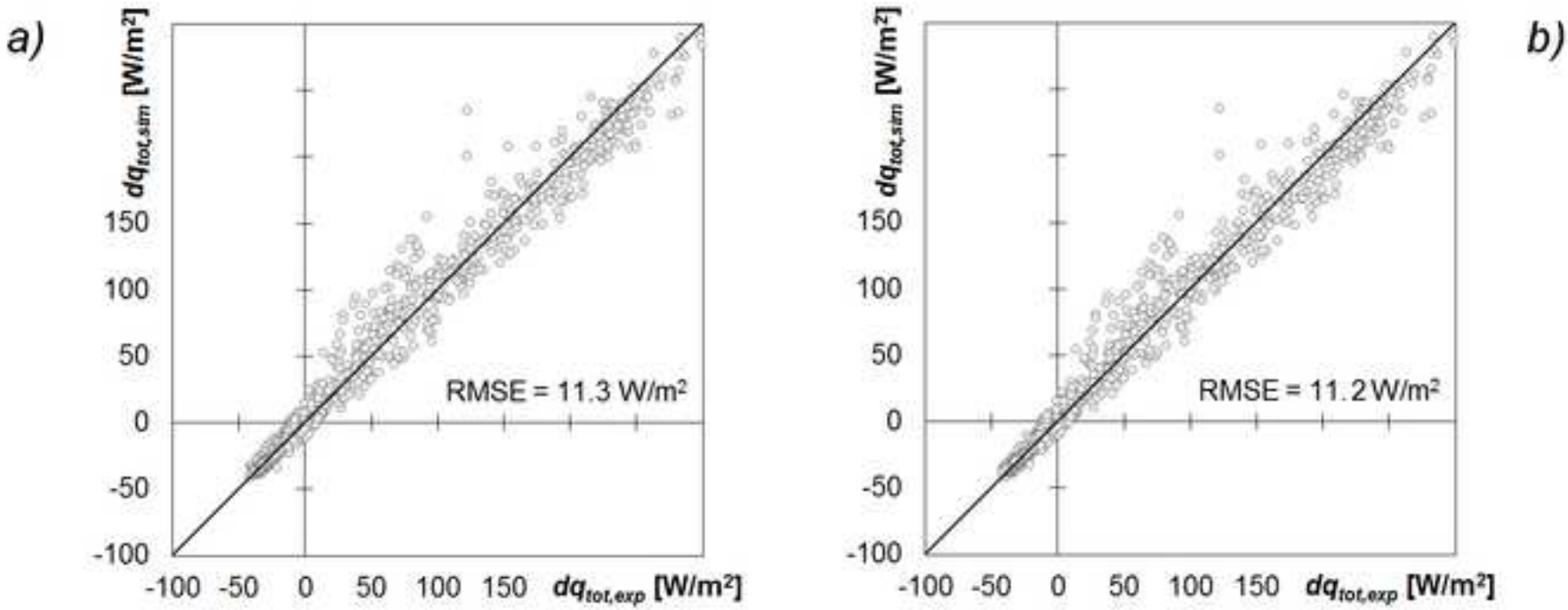

Figure 13

Click here to download high resolution image